



PII S0016-7037(99)00004-6

Re-Os systematics of mantle xenoliths from the East African Rift: Age, structure, and history of the Tanzanian craton

JOHN T. CHESLEY,^{1,*} ROBERTA L. RUDNICK,² and CIN-TY LEE²

¹Dept. of Geosciences, University of Arizona, Gould-Simpson Building #77, Tucson, AZ 85721, USA

²Dept. Earth and Planetary Sciences, Harvard University, 20 Oxford St., Cambridge, MA 02138, USA

(Received August 5, 1998; accepted in revised form January 1, 1999)

Abstract—In order to understand the effects of contractional and extensional tectonics on thick, mantle roots, we have undertaken a systematic study of mantle xenoliths from the Labait volcano, which lies within the East African Rift on the eastern boundary of the Archean Tanzanian craton. The Re-Os systematics of the Labait xenoliths show that ancient, refractory lithosphere is present to depths of ~140 km. Above this depth, the mantle section consists of harzburgitic xenoliths with whole rock ¹⁸⁷Os/¹⁸⁸Os between 0.1081 and 0.1140, corresponding to Re depletion (T_{RD}) ages of 2.8 to 2.0 Ga. Chromites from these samples are generally less radiogenic than their corresponding whole rocks and have T_{RD} ages between 2.5 to 2.9 Ga, yielding the best estimate for the age of this portion of the lithosphere. Coupled petrographic and isotopic data for some of these samples indicate they have been variably overprinted by recent addition of Re and/or radiogenic Os. Between 4.4 to 4.7 GPa (~140 to 150 km depth), peridotites are more fertile and yield younger T_{RD} ages (1.0 Ga to future ages). The highest temperature sample has radiogenic ¹⁸⁷Os/¹⁸⁸Os (0.133), overlapping the range measured for metasomatic xenoliths and the Labait host melilitite (0.13 to 0.14). This range is taken to represent asthenospheric mantle beneath the Tanzanian craton, which has plume-like isotopic characteristics. The suite shows a good correlation on ¹⁸⁷Os/¹⁸⁸Os vs. temperature (hence depth) and ¹⁸⁷Os/¹⁸⁸Os vs. wt.% Al₂O₃ or CaO plots. These trends, which pass above primitive mantle compositions, may reflect mixing of recent plume-derived Os with ancient lithospheric Os, formation of the lowest portion of the lithosphere during successive melting events or a combination of both processes.

Our data show that complete delamination of the lithospheric mantle has not occurred beneath the Tanzanian craton during its long tectonic history. However, if the Archean lithosphere was originally thicker than the ~140 km currently beneath Labait, then the lithosphere has been thinned, either by thermal erosion associated with the rift or by partial delamination during Proterozoic collision. Finally, we see no evidence for extensive lithospheric thinning associated with development of the East African Rift, although overprinting of the lithosphere by rift-related magmas has occurred. *Copyright © 1999 Elsevier Science Ltd*

1. INTRODUCTION

Over the last decade Re-Os isotopic studies have been applied with great success to understanding the timing of mantle lithosphere formation beneath the continents. To date, Re-Os studies of mantle xenoliths from four Archean cratons have been made: Kaapvaal (Carlson et al., 1999a; Olive et al., 1997; Pearson et al., 1995a; Walker et al., 1989), Siberia (Pearson et al., 1995b), Wyoming (Carlson and Irving, 1994, Carlson et al., 1999b) and Zimbabwe (Carlson, 1999a). Peridotites from these cratons typically show a range of Os isotopic compositions, from superchondritic ¹⁸⁷Os/¹⁸⁸Os, to unradiogenic values that are indicative of melt extraction in the early to middle Archean. In every case, the oldest rhenium-depletion model ages (T_{RD} ; these model ages represent minimum ages and assume no change in ¹⁸⁷Os/¹⁸⁸Os after time of melt depletion) approximate the ages of the oldest rocks in the overlying continental crust, implying that lithospheric mantle formation and crustal growth occurred simultaneously (at least within the resolving power of the Re-Os system, ca. 100 Ma). In addition, for most cratons there is no evidence from Re-Os systematics for loss of the mantle root. That is, there is no depth stratification to the Os

model ages, with the oldest ages randomly distributed both vertically and laterally within cratons. This observation suggests that once formed, these buoyant, refractory mantle roots remain intact for billions of years.

However, few Re-Os studies have yet to be undertaken in cratonic regions affected by rifting or post-cratonization collision—geodynamic settings in which erosion (Prodehl et al., 1994) or delamination (Houseman et al., 1981) of the cratonic mantle root may occur. An exception is a recent study from the Wyoming craton, (Carlson et al., 1999b), which shows that xenoliths derived from the greatest depths (150–170 km) have Os isotopic compositions overlapping those of abyssal peridotites, suggesting that these deep-seated samples may represent recent additions to the base of the lithosphere. If the original mantle root extended deeper than 150 km (which seismic studies suggest to be the case in other cratons), it implies that the lowest section of mantle lithosphere may have been lost beneath the Wyoming craton, perhaps during the late Mesozoic contractional orogeny that formed the Rocky Mountains (Carlson et al., 1999b). This study highlights the usefulness of the Re-Os system for documenting not only the timing of lithospheric formation, but perhaps also its destruction.

An unresolved issue in Re-Os studies is the interpretation of the young T_{RD} ages that are prevalent in cratonic xenolith suites. In some instances, these younger ages cluster around a

*Author to whom correspondence should be addressed (jchesley@geo.arizona.edu).

particular time period, such as the 2.0–2.3 Ga event recorded in xenoliths from the Premier kimberlite, South Africa, which have been interpreted as reflecting a Bushveld “imprint” on the cratonic mantle there (Carlson, 1999a). In most cases, however, the younger ages show no discernible clustering or regional patterns and have been interpreted as reflecting host infiltration, variable time-integrated Re/Os ratios and the influence of mantle metasomatism on Re/Os ratios (Pearson et al., 1995a; Pearson et al., 1995b; Walker et al., 1989).

In order to understand the effects of geodynamic processes on the stability of cratonic mantle and the origin of the young T_{RD} ages in cratonic xenolith suites we have undertaken a multi-faceted study of lithospheric mantle on the eastern border of the Tanzanian craton. This region is an ideal place to carry out such a study because it has experienced several episodes of compressional and extensional tectonism over its ~ 3 Ga history. These include subduction and collision during the formation of the ~ 2 Ga Usagaran belt, another episode of subduction and collision during the pan-African orogeny at ~ 700 Ma and finally, development of the East African rift, in the Cenozoic.

We have concentrated our initial efforts on xenoliths from the Pleistocene Labait volcano, which samples a wide range of mantle lithologies. Petrography, mineral chemistry, thermobarometry and whole rock major element compositions are reported for Labait xenoliths in Dawson et al. (1997) and Lee and Rudnick (1999). Here we report Re-Os and S measurements for whole rocks and minerals from Labait xenoliths and use these data to evaluate the age of the lithosphere, how it may have been affected by the long-lived tectonic history of the craton and the effects of metasomatism on the Re-Os system.

2. GEOLOGIC SETTING

Labait volcano sits on the boundary between the Tanzanian craton and Usagaran belt (Fig. 1). The Tanzanian craton, although still only poorly mapped, contains greenstone successions and late Archean granitoids. Rb-Sr whole rock isochrons from granitoids fall into two age groups: 2.74 and 2.54 Ga (Bell and Dodson, 1980), and Nd model ages range from 3.0 to 3.1 Ga (Möller et al., 1998), indicating a middle Archean crust formation age for the craton. The age of the greenstones is unknown.

The Archean craton is surrounded on all sides by Proterozoic mobile belts. Directly to the east of Labait lies the Usagaran belt, an early Proterozoic metamorphic belt (~ 2.0 Ga) that was subsequently metamorphosed during pan-African (615–650 Ma) collision (Möller et al., 1995). Recent Nd and Pb model ages for these rocks show them to be as old as those on the craton (2.7–3.3 Ga, Möller et al., 1998), implying that cratonic lithosphere extends some distance to the east of the currently exposed boundary. This is supported by Archean Nd model ages for metamorphic rocks in the eastern Mozambique belt (Möller et al., 1998) and by an Archean Re depletion model age for a peridotite xenolith from the Lashaine tuff cone (Burton et al., 1998), which lies ~ 150 km east of the craton in northern Tanzania.

Rifting developed in the Cenozoic, with the eastern arm of the east African rift propagating southwards from Kenya in the Neogene (Dawson, 1992). The well-defined rift valley in Kenya becomes more diffuse in northern Tanzania, where it splays

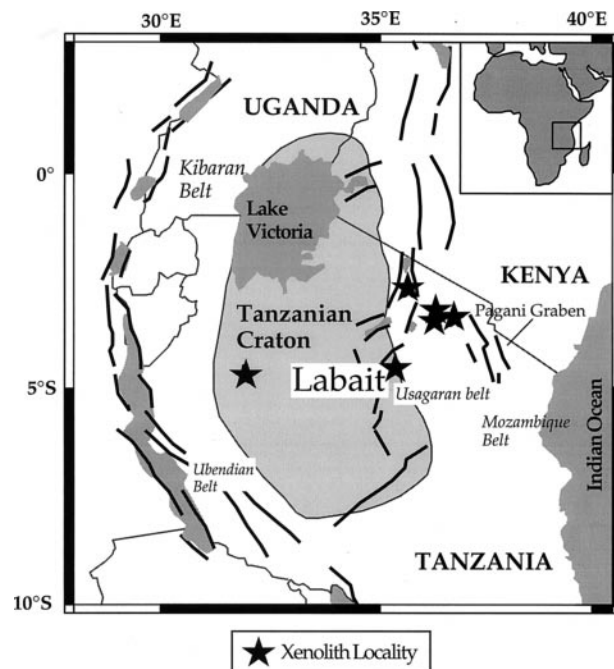


Fig. 1. Map of northern Tanzania showing the location of the Labait volcano and other xenolith-bearing rift volcanoes with respect to the East African rift, the boundary between the Tanzanian craton and the Usagaran belt.

into a wide zone of block faulting spanning ~ 300 km from east to west. It includes a series of NE striking normal faults and grabens, which extend 100–150 km into the eastern margin of the craton, and the Pagani graben, which lies ~ 250 km to the east in the Mozambique fold belt (Fig. 1). Seismicity and volcanism are confined to the western margin of this zone, in the vicinity of the boundary between the Tanzanian craton and Usagaran belt (Nyblade et al., 1996).

Geophysically, the Tanzanian craton is characterized by high elevation, a negative Bouguer gravity anomaly (Ebinger et al., 1997) and low heat flow (Nyblade et al., 1990). Results from a recent broad-band seismic experiment show that the Tanzanian mantle root is largely intact beneath the craton to depths of at least 200 km, that the uplift and negative gravity anomaly are due to hot, low density material beneath the cratonic root and that erosion and/or heating of this ancient root is confined to the vicinity of the rift (Ritsema et al., 1998). Our xenolith studies at Labait provide first-hand observations on how rifting is affecting this cratonic root.

3. SAMPLES

Mantle xenoliths from Labait include peridotites, pyroxenites and glimmerites. Peridotites span a wide range of compositions and mineralogies including spinel facies harzburgites and lherzolites, chromite-bearing harzburgites, garnet harzburgites and lherzolites as well as Fe-rich dunites (Lee and Rudnick, 1999; Appendix). In general, garnet-bearing lithologies are more fertile, having higher Al_2O_3 , CaO and lower Mg#, than the garnet-free harzburgites. The Fe-rich dunites may represent crystal cumulates or the product of melt-rock reaction

and, although they dominate the xenolith suite (constituting ~75% of the xenoliths present at Labait), we have concentrated our initial Re-Os efforts on the refractory peridotites in order to investigate the timing of lithosphere formation.

P-T estimates for the garnet peridotites fall in a scattered field near a geotherm of ~50 mW/m² (Dawson et al., 1997; Lee and Rudnick, 1999). There is an overall correlation between bulk composition and depth, with more fertile peridotites occurring at pressures greater than 4.4 GPa (~140 km; Lee and Rudnick, 1999). Trace element compositions in the Tanzanian xenoliths show LILE enrichments (Lee and Rudnick, unpublished data), similar to cratonic mantle xenoliths worldwide (McDonough and Frey, 1989). Several styles of pre-entrainment, metasomatic overprinting are recognized from petrography and whole rock geochemistry: (1) Fe-enrichment without development of obvious secondary phases, (2) formation of secondary clinopyroxene in melt pockets and rimming chromite, (3) overprinting by high-field-strength element rich melts (precipitating phlogopite ± ilmenite ± rutile ± sulfide ± zircon), and (4) rare carbonate precipitation (Lee and Rudnick, 1999). It is unclear how these different styles of metasomatism relate to one another in space and time, although at least one stage of metasomatism is rift-related, based on U-Pb dating of Pleistocene zircons (400 ± 200 Ka) in an Fe-rich, metasomatic vein (sample LB-17, Rudnick et al., 1999).

The ¹⁸⁷Os/¹⁸⁸Os and Re, Os and S concentrations were determined for a subset of the 39 mantle xenoliths described in Lee and Rudnick (1999), chosen to span the range of observed compositions. We have divided these into three groups: (1) refractory peridotites consisting of one spinel facies harzburgite, six garnet harzburgites, two garnet lherzolites and six garnet-free, chromite-bearing harzburgites, (2) four Fe-rich dunites and (3) xenoliths that represent metasomatic additions to the lithosphere: one pyroxenite and one glimmerite. Of these samples, one of the refractory peridotites, garnet lherzolite LB-45, bears special attention. This sample, although still refractory (as witnessed by its forsterite content of Fo_{90.2}), contains appreciable clinopyroxene (~15%) and has a major element composition approaching estimates of the primitive mantle (e.g., McDonough and Sun, 1995). This sample also has the highest equilibration temperature of the suite (~1400°C), and, like the other high temperature garnet peridotites, has a deformed texture (see Appendix).

In addition to these whole rock measurements, the Os isotopic compositions of chromite, spinel and sulfide separates were determined in order to estimate the initial ¹⁸⁷Os/¹⁸⁸Os of the peridotites and delineate the effects of mantle metasomatism on whole rock compositions. Finally, the host lava was measured in order to define the Os isotopic composition of rift-related magmas and to help evaluate the effects of melt infiltration on the Os isotopic system.

4. ANALYTICAL TECHNIQUES

Whole rock powders were prepared by first crushing the rock between plastic sheets with a rock hammer. Fragments devoid of weathering rind and host lava were then processed first through an alumina jaw crusher and then through an alumina disk mill. The fine material from the disk mill was then split through an aluminum sample splitter. Approximately half was then pulverized in an alumina ring mill, the remaining half was reserved for the preparation of mineral separates.

Chromite and sulfide separates were concentrated using standard heavy liquid and magnetic techniques and then hand-picked. Chromite samples were abraded and then ground in an agate mortar and pestle.

Whole rock samples were spiked with ¹⁸⁵Re and ¹⁹⁰Os; dissolution of the rocks and equilibration of spike and sample were achieved using a modified Carius tube technique (Shirey and Walker, 1995). Whole rock samples (0.5 to 2 g) were loaded in a Carius tube with 6–12 ml of 2:1 HNO₃:HCl and heated at 240°C for at least 24 hours. Approximately 50 to 300 mg of crushed chromite separate or chromite powder resulting from abrasion was dissolved, unspiked, in two stages: the first stage in 2 ml of 12N HCl and the second in 4 ml concentrated HNO₃ (the Carius tube was broken and resealed for the second acid addition before heating at 210°C). Os was separated and purified using a modified organic separation procedure (Cohen and Waters, 1996), utilizing 3 separate extractions, with ~90% recovery of Os (Chesley and Ruiz, 1998). The Os total processing blank was <1 pg and is inconsequential in all samples. The remaining Carius tube liquid was dried and Re was separated and purified from this using two successive anion exchange columns (200–400 mesh) with resin volumes of 0.3 and 0.1 ml, respectively. The samples were loaded and eluted on columns using 0.1 N HNO₃, Re was then collected using 8 M HNO₃, and then dried under heat lamps (<80°C). Samples were corrected for Re blanks of 7 pg. Purified Re and Os were then loaded using BaSO₄ and Ba(OH)₂ as emission enhancers, respectively, on platinum filaments and analyzed using negative thermal ionization mass spectrometry (after Creaser et al., 1991; Volkening et al., 1991; Chesley and Ruiz, 1998). Duplicate analyses of samples show good reproducibility (Table 1 and Table 2).

Re depletion (T_{RD}) ages were calculated assuming that the melt depletion event removed all of the Re (the Re/Os ratio is therefore zero) and any measured Re is secondary (Walker et al., 1989); T_{RD} ages therefore represent minimum ages of melt withdrawal. We used primitive mantle values of ¹⁸⁷Re/¹⁸⁸Os = 0.401, ¹⁸⁷Os/¹⁸⁸Os = 0.1270 (e.g., Pearson et al., 1995a) ¹⁸⁷Re decay constant (λ) of 1.666E-11 (e.g., Shirey and Walker, 1998).

Sulfur analyses were carried out by K. Sharkey, University of Leicester, using a Leco determinator. Samples are weighed into a crucible with Fe and W chips added as accelerators to ensure complete combustion of the sample. The crucible is then heated in an R.F. induction furnace in a stream of O₂ and the sulfur derived as gaseous SO₂ and SO₃. The gases are then passed through a dust filter, drying tube [SO₂ dissolves in water, thus water must be removed] and finally through a catalyst tube to ensure conversion to dioxides. From there the gases go into the sulfur I.R. absorption cell and are passed through another tube that traps the SO₂ as SO₃. The SO₂ peak is then converted to S values. These values are then adjusted for calibration and sample weight to give the final concentration. The values reported in Table 1 represent the average of two separate analyses for each sample. Blank and standards are determined in the same manner as samples. Blanks (~0.3 ppm) are then subtracted from the sample.

5. RESULTS

Re-Os and sulfur data are presented in Tables 1 and 2 and are plotted in Figs. 2 to 4. Whole rock Os concentrations range from 0.5 to 5 ppb in the refractory peridotites, with the garnet-free samples generally showing the highest Os concentrations and the garnet-bearing samples the lowest. Interestingly, the Fe-rich dunites have Os concentrations that span most of the range of the refractory peridotites (Fig. 2). This range is typical of peridotite xenoliths elsewhere, as shown by the average Os values for Siberia, Kaapvaal and Wyoming. The two metasomatic xenoliths show low Os contents (0.4 to 0.7 ppb), which are matched only by one garnet harzburgite (LB-53 at 0.46 ppb).

Re concentrations range from 0.037 to 0.54 ppb in the refractory peridotites, with the garnet-bearing samples tending to have higher Re concentrations than garnet-free samples. The two garnet harzburgites that bear chemical and petrographic

Table 1. Whole rock Re-Os results for Tanzanian mantle xenoliths.

Sample	Re (ng/g)	Os (ng/g)	$^{187}\text{Re}/$ ^{188}Os	$^{187}\text{Os}/$ ^{188}Os	T_{MA} (Ga) [†]	T_{RD} (Ga)	T (°C)*	Fo	Al ₂ O ₃ wt.%	S ppm
Spinel-facies Harzburgites										
LB-11	0.037	1.262	0.1376	0.1119 (2)	3.40	2.24	990	92.3	0.84	—
Garnet-free Harzburgites										
LB-1	0.079	2.553	0.1470	0.1098 (3)	4.00	2.53		92.1	0.40	0.03
Repeat		2.545		0.1099 (2)						
LB-9	0.283	2.433	0.5600	0.1102 (4)		2.49		93.3	0.36	0.3
LB-14	0.058	4.851	0.0566	0.1081 (1)	3.25	2.80	990	92.9	0.33	0.6
LB-16	0.149	0.759	0.9416	0.1107 (3)		2.42	1260	91.9	0.60	—
LB-17	0.193	2.038	0.3198	0.1120 (2)		2.23	1070	91.1	0.56	0.2
KAT-1	0.011	3.348	0.015	0.1140 (1)		1.98		92.5	0.65	0.03
Garnet Harzburgites and Lherzolites										
LB-4	0.175	2.595	0.3198	0.1248 (2)	1.73	0.34	1340	91.3	1.54	0.5
LB-12	0.148	1.588	0.4424	0.1249 (3)		0.33	1290	90.6	1.98	0.6
Unspiked repeat			0.1247 (3)							
LB-24	0.164	1.406	0.562	0.1122 (2)		2.20	1268	92.4	1.21	0.2
LB-34	0.404	1.462	1.330	0.1103 (3)		2.48	1115	89.9	0.68	—
LB-45	0.545	1.119	2.349	0.1329 (2)	0.18	Future	1406	90.2	3.89	0.3
LB-50	0.086	1.757	0.233	0.1205 (4)	2.34	0.98	1359	91.2	1.37	—
LB-53	0.100	0.462	1.044	0.1223 (4)		0.71	1298	91.1	1.73	—
KAT-17	0.342	1.418	1.165	0.1247 (3)		0.36	1240	89.0	0.41	—
Fe-rich Dunites										
KAT-5	0.373	2.895	0.621	0.1194 (2)		1.15		86.4	—	0.5
KAT-12	0.340	1.374	1.190	0.1154 (5)		1.73		85.9	—	—
KAT-14	0.182	1.955	0.457	0.2537 (4)		Future		86.7	—	—
LB-59	0.364	0.926	1.897	0.1287 (3)	0.06	Future		85.1	—	—
Metasomatic Xenoliths										
LB-15, Pyroxenite	0.144	0.741	0.9369	0.1386 (2)	1.27	Future		86.3	1.23	—
LB-49, Glimmerite	0.036	0.422	0.4125	0.1320 (3)		Future			12.92	0.5
Melilitite				0.1387 (2)		Future				

— in sulfur column means below detection, — in other columns means not measured. [†] Blanks represent T_{MA} 's that are older than 4.5 Ga. * Samples for which no temperatures are reported lack primary clinopyroxene, orthopyroxene or both. T_{MA} : Os model age calculated using observed Re/Os of the sample, primitive mantle $^{187}\text{Re}/^{188}\text{Os} = 0.397$ and $^{187}\text{Os}/^{188}\text{Os} = 0.12705$. T_{RD} ages assume no Re in the sample. Numbers in () after Os isotopic compositions are 2σ errors.

evidence of Fe-enrichment (LB-34 and KAT-17, see Lee and Rudnick, 1999) have considerably higher Re contents than most of the other refractory peridotites (0.34–0.40 ppb cf.

Table 2. Re-Os results for chromites and sulfide separates from Tanzanian mantle xenoliths.

Sample #	Re (ng/g)	Os (ng/g)	$^{187}\text{Re}/$ ^{188}Os	$^{187}\text{Os}/$ ^{188}Os	T_{RD} (Ga)
SULFIDE*					
LB-12				0.1242	0.42
CHROMITES					
LB-11, spinel #				0.1142	1.91
spinel powder				0.1158	1.68
LB-1 chromite				0.1076	2.87
repeat				0.1074	
LB-9 chromite #				0.1083	2.77
LB-16 chromite #				0.1100	2.52
LB-17 chromite				0.1183	1.31
chromite powder				0.1296	Future
KAT-1 chromite (not abraded)	0.094	59	0.008	0.1093	2.67

* Sulfides in this and other samples are monosulfide solid solution, showing variable degrees of exsolution and sometimes intergrown with Fe-oxides. Chalcopyrite exsolutions are rare. "Chromite" refers to abraded cores. "Chromite powder" refers to the powder derived from the abrasion of the chromites. # \pm variation on repeat measurement from the same Os extraction less than 0.0001.

0.037–0.280 ppb), giving them high Re/Os (Fig. 2). The relatively fertile lherzolite, LB-45, is the exception to this generalization and has the highest Re concentration and Re/Os of the suite. The Fe-rich dunites have relatively high Os (0.9 to 2.9 ppb) and Re contents (0.18–0.37 ppb) and variable Re/Os. The $^{187}\text{Re}/^{188}\text{Os}$ ratios of the suite range from subchondritic to superchondritic (0.01 to 2.3). Interestingly, the two metasomatic xenoliths have low Re contents and, consequently, low Re/Os ratios; the glimmerite has one of the lowest Re contents of the suite (0.036 ppb).

Os isotopic ratios are highly variable in the refractory peridotites, with $^{187}\text{Os}/^{188}\text{Os}$ ranging from 0.1081 to 0.1329, corresponding to Re depletion (T_{RD}) model ages of 2.8 Ga to the future, respectively (Fig. 3, Table 1). The Os isotopic composition does not correlate with Re/Os (Fig. 3), but correlates with both overall fertility (as reflected in whole rock Al₂O₃ and CaO contents and forsterite contents) and equilibration temperature (Fig. 4). One sample, KAT-17, deviates significantly from these trends. This sample is Fe-rich and Al- and Ca-depleted and does not fall on partial melting trends defined by the other samples (Lee and Rudnick, 1999). These features lead us to conclude that this sample has undergone post-formational changes (perhaps mechanical removal of garnet and/or Fe-enrichment) that cause it to fall off of the trends, and it will therefore not be considered in the following discussions.

Sulfur is incompatible during mantle melting and is expected

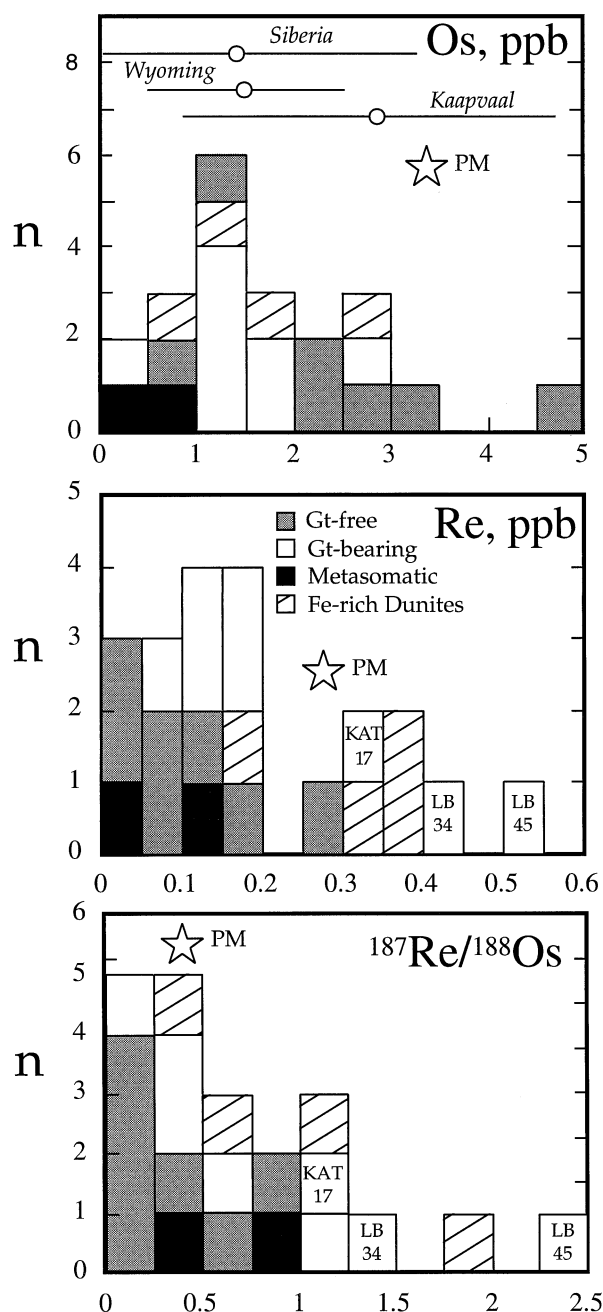


Fig. 2. Os and Re concentration and Re/Os histograms showing data for garnet-bearing and garnet-free refractory peridotites, Fe-rich dunites and metasomatic xenoliths (glimmerite and pyroxenite) from Labait, Tanzania. Circles and bars in upper diagram show the mean and standard deviation of Os concentrations for kimberlite-hosted xenoliths from the Siberian and Kaapvaal cratons (Pearson et al., 1995; Walker et al., 1989; Olive et al., 1997) and minette-hosted xenoliths from the Wyoming craton (Carlson and Irving, 1994). The two Fe-enriched garnet peridotites (KAT-17 and LB-34) also show the highest Re concentrations of the refractory peridotites, suggesting that Fe enrichment is accompanied by Re addition. Sample LB-45 has major element composition similar to the primitive mantle. Note that the Fe-rich dunites have Os contents indistinguishable from the refractory peridotites, but generally higher Re contents, consistent with their formation via melt-rock reaction. Two sigma errors are smaller than the data points in all cases.

to be significantly lower in refractory peridotites (like many of the Labait xenoliths) compared to the primitive mantle (250 ppm, McDonough and Sun, 1995). For example, sulfur contents lie between 7 and 55 ppm for peridotites having 45% MgO from the Pyrenees ultramafic massifs (Lorand, 1989). Sulfur concentrations are extremely low in the Labait xenoliths, ranging from <1 ppm to below detection limits (Table 1). Not all Labait xenoliths are refractory, yet even the more fertile ones have very low sulfur contents (Burnham et al., 1998) (e.g., LB-45, which has a primitive mantle-like major element composition has only 0.3 ppm S). Moreover, S concentration does not correlate with indicators of melt depletion, such as MgO concentration. These observations suggest that sulfur has been lost from the xenoliths after the original melt depletion event, perhaps by breakdown of primary sulfides to iron oxides during decompression of the xenoliths (Lorand, 1990). As most of the Os (and other PGE's) are likely to be hosted in sulfides in fertile peridotites (Hart and Ravizza, 1996), it is not clear how this breakdown may have affected Os contents. The very low Os in some samples (e.g., LB-53) might be explained in this way. In one garnet peridotite (LB-12) we have observed Pt alloy associated with Fe oxide breakdown products, suggesting that at least some of the PGE's are retained during sulfide decomposition (see also Keays et al., 1981).

Analyses of sulfides, spinels, abraded chromites and the resulting powder are listed in Table 2. In most samples the chromites are less radiogenic than the whole rocks, indicating a lower time-integrated Re/Os. This is verified in the single chromite for which Re and Os concentrations have been determined (KAT-1, Table 2) and is consistent with previous studies documenting high Os and low Re concentrations in chromites (Marcantonio et al., 1993; McCandless and Ruiz, 1991). However, two samples show the opposite relationship: LB-17 and LB-11; moreover, the abraded rims of the chromites and spinels in these samples are more radiogenic than the cores. Sample LB-17 has an Fe-rich vein containing orthopyroxene, chromite, rutile, sulfide and zircon, the latter of which has been dated by the U-Pb method at 400 ± 200 Ka (Rudnick et al., 1999). Chromites in this vein are riddled with inclusions, including sulfides (Fig. 5). Sample LB-11 is one of the few spinel-facies peridotites in our collection. The spinels in this sample show euhedral overgrowths and are often surrounded by glass pockets that contain sulfide. The Os isotopic composition of the sulfide separate from a garnet lherzolite is indistinguishable from that of the whole rock (Tables 1 and 2).

The Os isotopic composition of the host melilitite (taken from a lava rind on one of the peridotite bombs) is radiogenic ($^{187}\text{Os}/^{188}\text{Os} = 0.1387$, Table 1) compared to the mantle peridotites. The presence of dense peridotite xenoliths in a lava is generally cited as evidence for the extremely rapid eruption of this magma from upper mantle depths (Spera, 1980), minimizing chances of interaction of the magma with Archean continental crust. The $^{187}\text{Os}/^{188}\text{Os}$ is also very low compared to other lavas that have been shown to have undergone significant crustal interaction (e.g., Chesley and Ruiz, 1998). This Os isotopic composition is therefore the best estimate we have for the mantle source of the rift volcanics and overlaps that of plume-derived, ocean island magmas (see Shirey and Walker, 1998, and references therein).

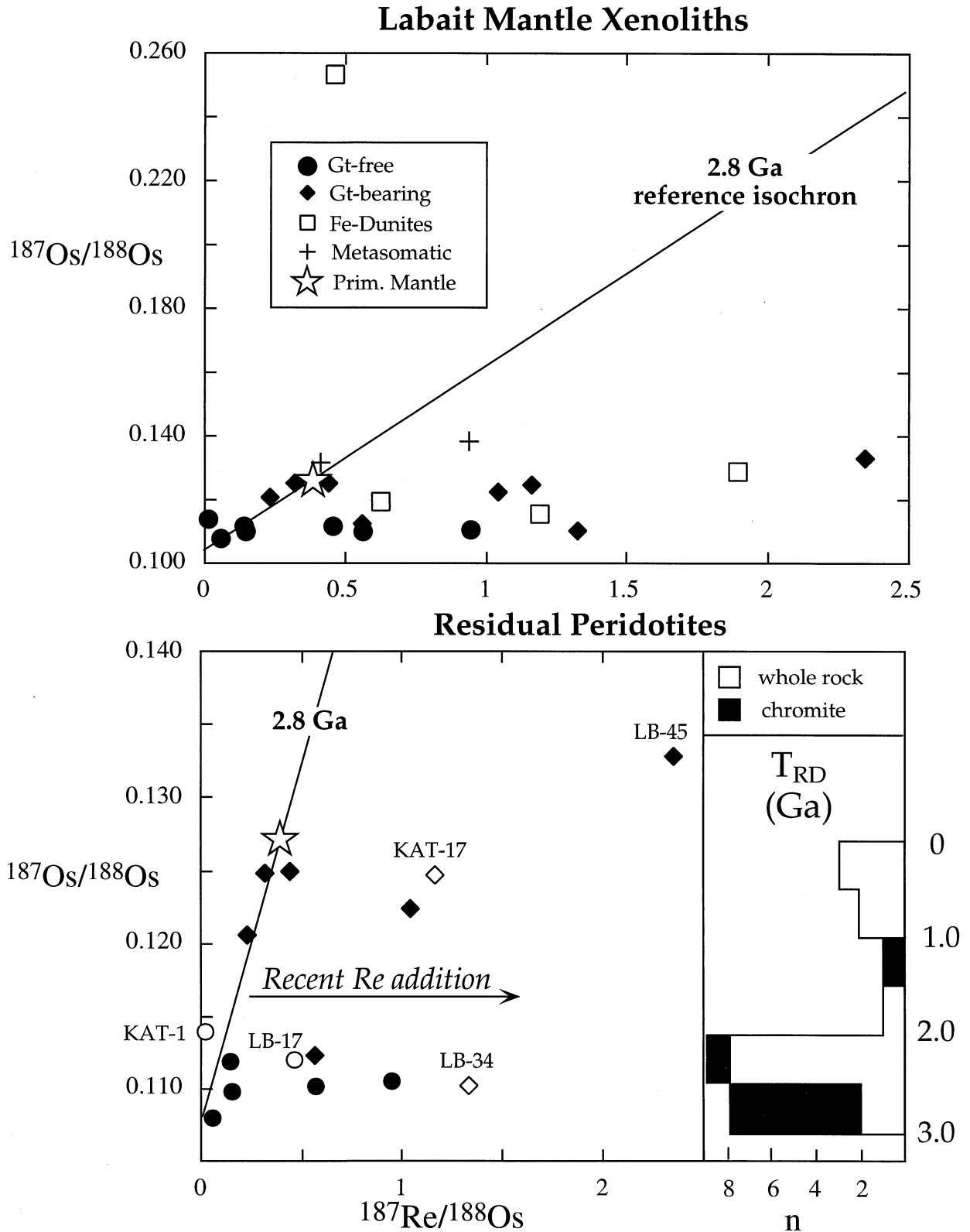


Fig. 3. Re-Os isochron plots. *Upper*: All mantle xenoliths from Labait. A 2.8 Ga isochron is plotted for reference. Star is the primitive upper mantle composition (McDonough and Sun, 1995; Pearson et al., 1995). Only the two metasomatic xenoliths (a glimmerite and a pyroxenite), one Fe-rich dunite and sample LB-45 are more radiogenic than primitive mantle. *Lower*: Residual peridotites; Re-depletion model ages are plotted as histogram on right axis. The two garnet-bearing peridotites plotted as open diamonds (KAT-17 and LB-34) and garnet-free peridotite LB-17 (open circle) show geochemical and petrographic evidence for recent Fe-enrichment. KAT-1 (open circle) has chromite that is markedly less radiogenic (Table 2, Fig. 6). Both KAT-1 and LB-17 show evidence of recent radiogenic Os addition (see text).

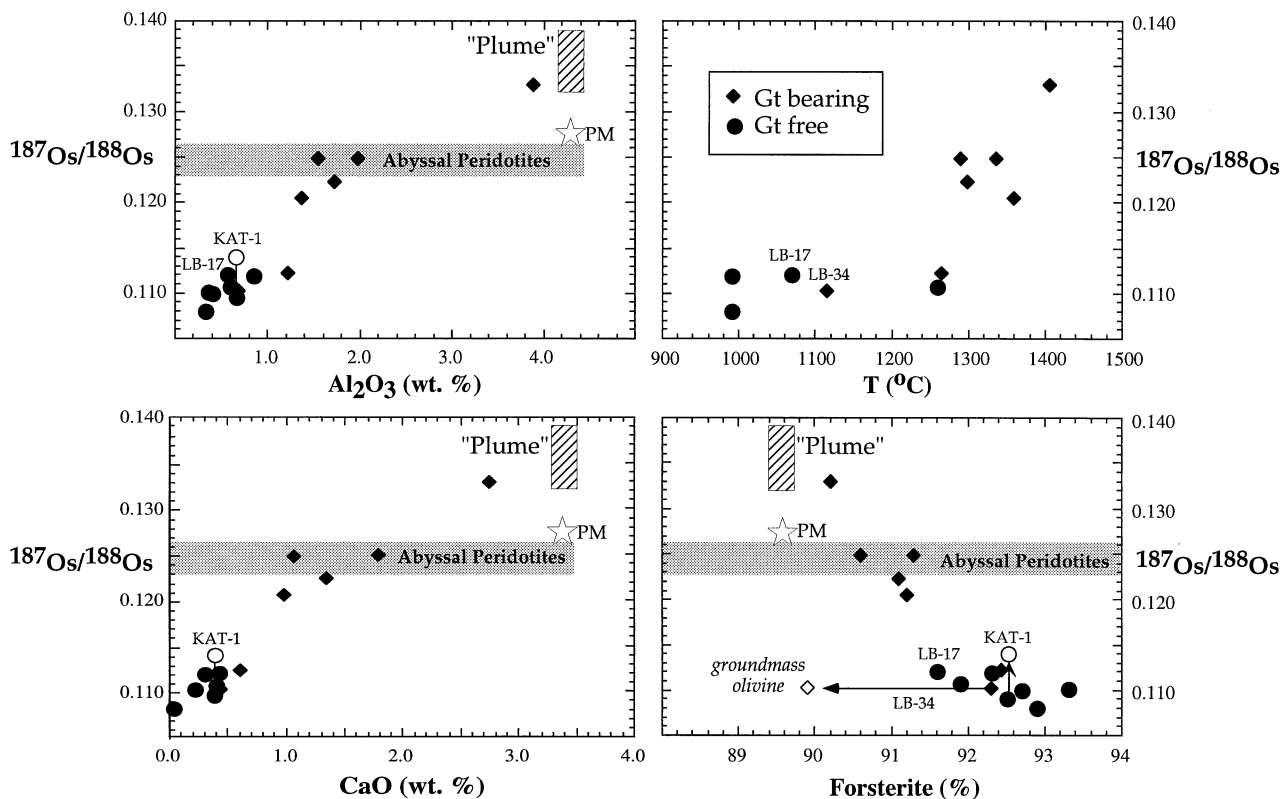


Fig. 4. Al_2O_3 , CaO, equilibration temperature and forsterite content vs. $^{187}\text{Os}/^{188}\text{Os}$. The data follow a positive correlation in the Al and Ca plots and a negative correlation on the Fo plot, but the trends do not pass through the primitive mantle composition (marked by a star), indicating that they are not simply due to a *single* partial melting event. $^{187}\text{Os}/^{188}\text{Os}$ of abyssal peridotites is from Roy-Barmen and Allègre (1995) and Snow and Reisberg (1995). Box with diagonal shading marked "Plume" represents range of $^{187}\text{Os}/^{188}\text{Os}$ of metasomatic xenoliths and host melilitite shown with primitive mantle-like major element compositions. Garnet-free peridotites KAT-1 and LB-17 show evidence for recent addition of radiogenic Os (see text). Sample LB-34 experienced recent Fe and Re addition. The open symbol for this sample shows the forsterite content of groundmass olivine, the closed symbol shows the forsterite content of an olivine inclusion inside garnet. The processes responsible for this Fe-enrichment apparently did not affect the bulk rock Al and Ca contents or Os isotopic composition. Temperatures calculated using the Brey and Kohler (1990) two pyroxene thermometer (see Lee and Rudnick, 1999).

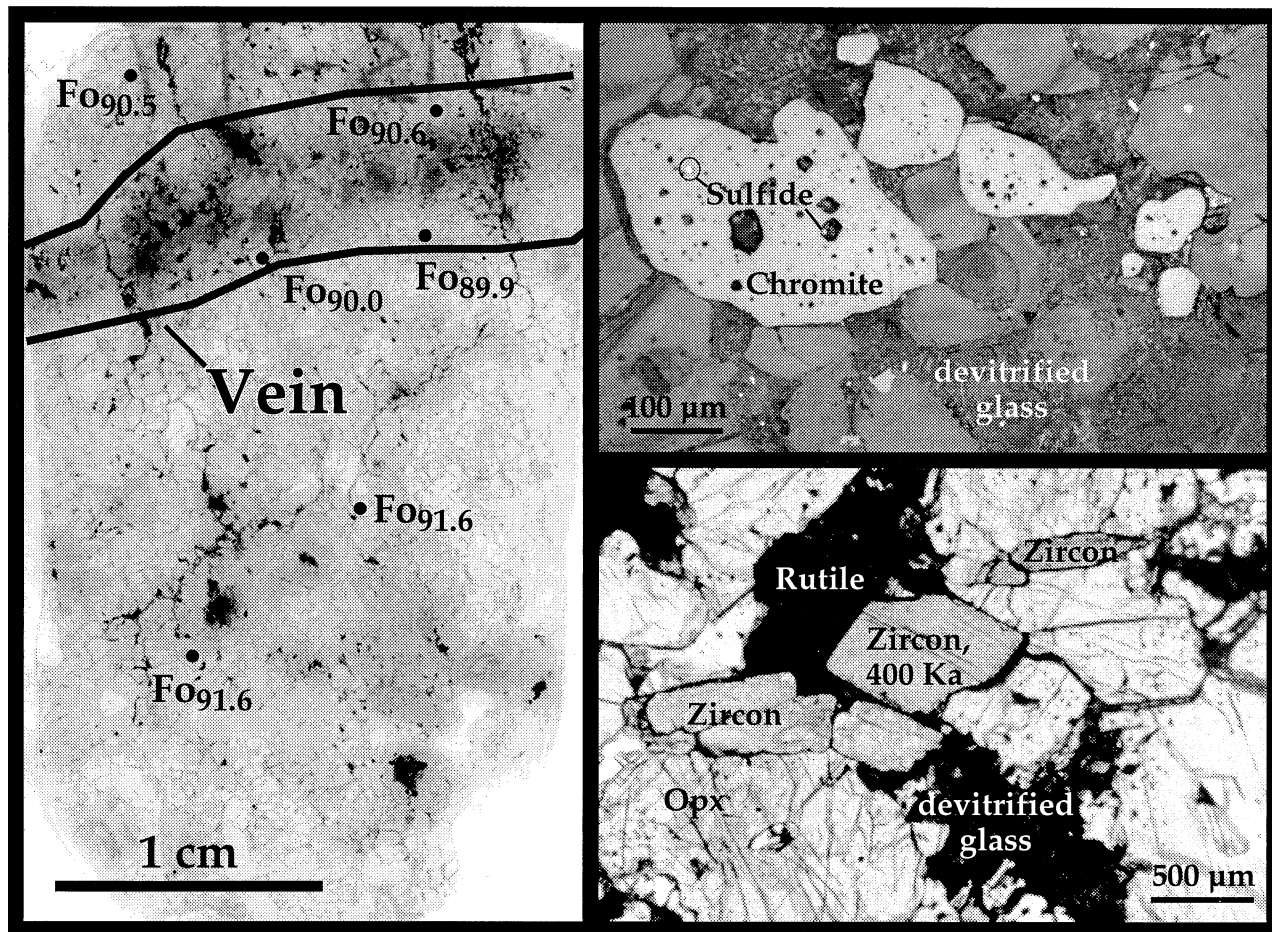
6. METASOMATIC EFFECTS ON RE-OS SYSTEMATICS

Recent Re-Os studies of mantle xenoliths have been carried out on samples showing both cryptic and modal metasomatism in order to evaluate how these chemical and mineralogical changes may have affected the Re-Os system. Brandon et al. (1996) suggested that LILE-enriched mantle xenoliths occurring in a back-arc setting had seen addition of radiogenic Os from slab-derived fluids. In a study of peridotite xenoliths from S.E. Australia, Handler et al. (1997) found no change in Re/Os or $^{187}\text{Os}/^{188}\text{Os}$ associated with carbonatite metasomatism, which is manifested as formation of secondary clinopyroxene and apatite and enhancement of CaO and depletion of Al_2O_3 in refractory peridotite. Olive et al. (1997) also found no change in either Re/Os or $^{187}\text{Os}/^{188}\text{Os}$ in refractory cratonic peridotites from Lesotho that experienced Fe-enrichment adjacent to pyroxenite dikes, nor did they see any significant changes in Re-Os systematics in a particular type of high-field-strength element rich vein (referred to as IRPS, for Ilmenite, Rutile, Phlogopite and Sulfide) and host peridotite. They did, however, see elevated Re/Os ratios and more radiogenic $^{187}\text{Os}/^{188}\text{Os}$ in pyroxenite dikes.

We have attempted to determine the Os isotopic compositions of potential metasomatic end members (Table 1): a glimmerite, a pyroxenite and the host lava. These samples all have $^{187}\text{Os}/^{188}\text{Os}$ ratios between 0.13 and 0.14, overlapping that of the highest temperature and most fertile peridotite, LB-45. This Os isotope composition is more radiogenic in Os than abyssal peridotites (generally assumed to represent depleted upper mantle—MORB source, Snow and Reisberg, 1995, Roy-Barmen and Allègre, 1995) and overlaps that of plume-derived, ocean island magmas (see Shirey and Walker, 1998, and references therein). These observations suggest that (1) the metasomatic xenoliths formed from rift-related magmas, (2) the sublithospheric mantle beneath the East African Rift has radiogenic Os isotopic characteristics similar to that of oceanic plumes, quite distinct from depleted oceanic mantle, and (3) lherzolite LB-45, which has the highest equilibration temperature ($\sim 1400^\circ\text{C}$), a deformed microstructure and a major element composition approaching primitive mantle, may be a sample of this plume-like mantle.

With the Os isotopic characteristics of rift-related magmas thus inferred, we now investigate how their passage may have

LB-17



$^{187}\text{Os}/^{188}\text{Os}$ Results

Whole rock = 0.112
Abraded Chromite = 0.118
Powdered Chromite = 0.130

Fig. 5. *Left*: Scan of LB-17 thin section showing diffuse vein containing orthopyroxene, rutile, chromite, zircon, sulfides, and devitrified glass. The vein is characterized by Fe-enrichment and abundant CO_2 fluid inclusions, which impart a dark coloration in the scanned image. *Top right*: Chromite from vein with myriad hollow inclusions, interpreted to have been filled with CO_2 . Sulfide occurs as a daughter phase in the CO_2 -rich fluid inclusions and as discrete inclusions. Similar textures have been described previously by Andersen et al. (1987). Sulfide also occurs as abundant inclusions within vein orthopyroxene. *Bottom right*: Large, euhedral zircons and rutiles from vein.

affected the Os isotopic characteristics of the ancient lithospheric mantle. In contrast to the previous studies cited above, our results for the Labait xenoliths document both Re-enrichment and changes in $^{187}\text{Os}/^{188}\text{Os}$ that are correlated with chemical and petrographic evidence of metasomatism. Iron and rhenium enrichment are seen clearly in two samples: garnet-peridotite LB-34 and garnet-free peridotite LB-17. In addition, LB-17 shows evidence for addition of radiogenic Os. More-

over, garnet-free peridotite, KAT-1, shows evidence for radiogenic Os addition without Fe or Re-addition. Each is discussed in turn.

6.1. Re-enrichment

Sample LB-34 has next to the highest Re/Os ratio amongst the refractory peridotites (Fig. 2) and also has higher FeO (9.3

KAT-1

LB-12

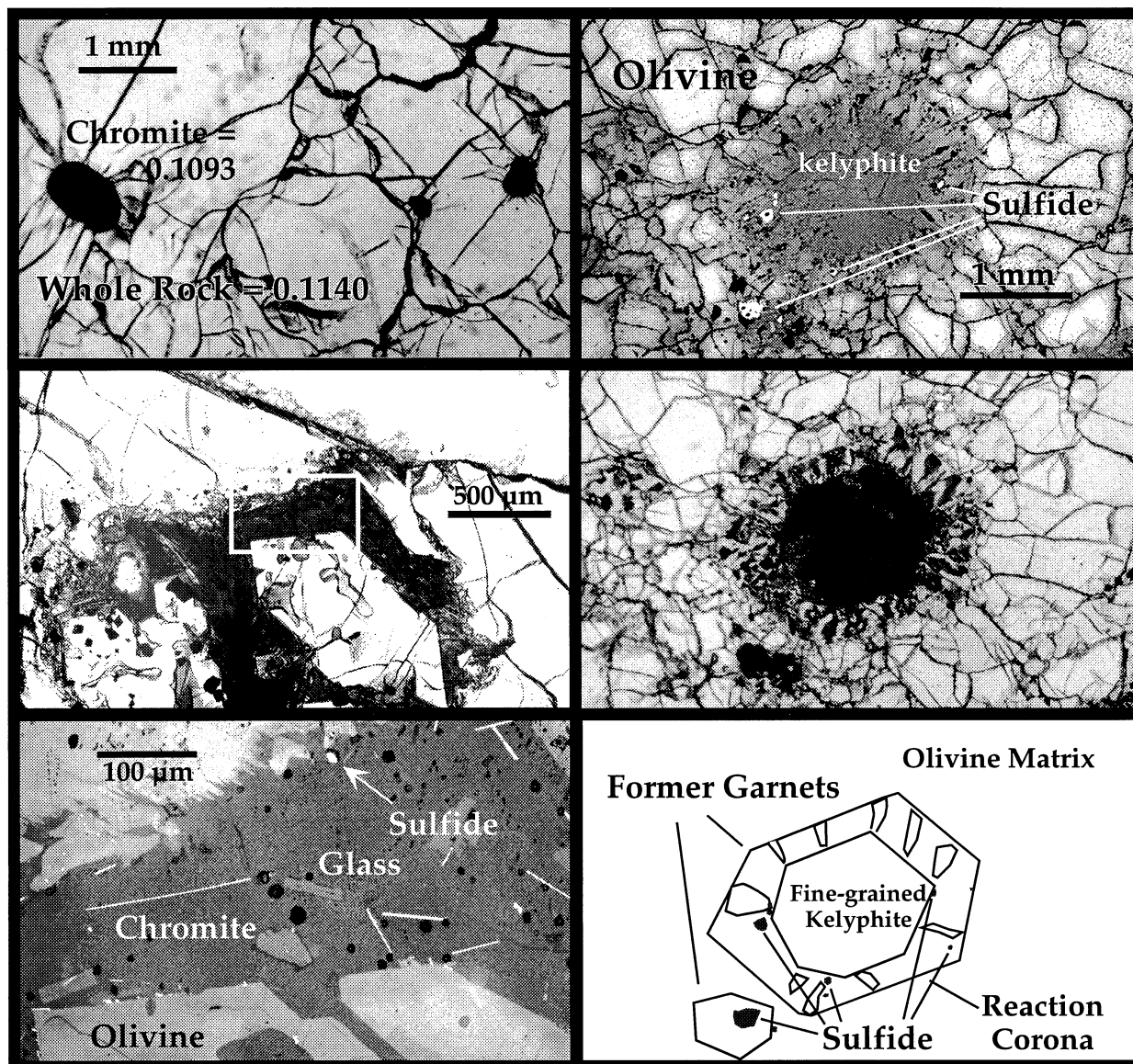


Fig. 6. *Left, upper*: Transmitted light photomicrograph of KAT-1 showing round, primary chromites having 50 ppb Os and unradiogenic Os compositions. *Middle*: Transmitted light photomicrograph of metasomatic glass patch with large, euhedral olivine. White box outlines field of view in bottom figure. *Bottom*: Reflected light photomicrograph showing phases in glass patch, including acicular chromites, euhedral olivines and round sulfides. *Right, upper*: Reflected light photomicrograph of LB-12 showing garnet breakdown patches in olivine matrix. Patches consist of an outer, coarse-grained corona of spinel and pyroxene and an inner, fine-grained core of kelyphite. The corona assemblage is interpreted to have formed at high P and T, prior to entrainment of the xenolith in the host melilitite. The fine-grained kelyphite is interpreted to have formed upon decompression in the pipe (see Lee and Rudnick, 1999). Sulfides (bright) are confined to the corona and are interpreted to have been introduced during the corona-forming reaction. Small black holes in sulfides are laser ablation pits (Lee et al., in prep). Platinum-alloys associated with development of Fe oxides have been observed in similar appearing sulfides. *Middle*: Transmitted light photomicrograph of the same garnet patch. *Bottom*: Sketch of garnet patch.

wt.%) and Re (0.4 ppb) contents than primitive mantle values (e.g., McDonough and Sun, 1995; Shirey and Walker 1998). It does not lie on the FeO vs. MgO trend defined by the other peridotites (Lee and Rudnick, 1999). This sample has definitive petrographic evidence for Fe-enrichment: an olivine inclusion inside former garnet has markedly higher Fo content than the

groundmass olivines (92.4 vs. 89.9, respectively, Fig. 4, Lee and Rudnick, 1999). These chemical and petrographic observations indicate that this sample experienced Fe-enrichment without appreciable changes to other major element oxides—it falls on the partial melting trends defined by the Al_2O_3 and CaO vs. MgO plots (Lee and Rudnick, 1999). The elevated Re

and Re/Os in this sample suggests that Re was added, in addition to Fe. This Fe and Re-enrichment may have occurred through diffusive exchange between the peridotite and an Fe- and Re-rich silicate melt prior to entrainment. The abundant Fe-rich dunites, which have relatively high Os and Re contents and low Mg# may also be products of such melt-rock interaction.

A second sample, LB-17, is cut by an orthopyroxene-rich vein (described previously). Groundmass olivines become more Fe-rich near the vein (Fo_{92} beyond ~ 4 mm from the vein and Fo_{90} adjacent to the vein), indicating that the melt that produced the vein imparted an Fe-enrichment to the wall rocks (Fig. 5). The moderately elevated $^{187}\text{Re}/^{188}\text{Os}$ of this sample suggests that Re was added in addition to Fe, as in LB-34 described above.

For samples lacking petrographic or chemical evidence for Fe enrichment, it is not as easy to determine whether Re enrichment has occurred. The fact that more than half of the residual peridotites have $^{187}\text{Re}/^{188}\text{Os}$ greater than primitive mantle, yet lower $^{187}\text{Os}/^{188}\text{Os}$ (Fig. 3b), suggests either recent Re addition or recent Os loss. The low Os concentration in some samples (e.g., garnet harzburgite LB-53) is indicative of Os loss, possibly due to sulfide breakdown upon decompression, as discussed above. However, recent Re addition is also probable in samples that have Re contents near or above the estimate of primitive mantle (e.g., LB-9, LB-34, KAT-17, LB-45).

6.2. Addition of Radiogenic Os

A second, perhaps related, style of metasomatism occurs in sample LB-17. As described in the previous section, this harzburgite contains a diffuse vein of Fe-rich orthopyroxene, rutile, phlogopite, chromite, zircon and sulfide that formed at 400 Ka, obviously a product of rift-related metasomatism. The style of metasomatism observed in the vein is somewhat similar to the IRPS metasomatism described from the Lesotho xenoliths (Olive et al., 1997), except that LB-17 has no discrete ilmenite (ilmenite occurs only as exsolution lamellae in rutile). The chromites in this sample, both groundmass and vein, have skeletal habits and are riddled with inclusions, but sulfide inclusions were observed only in chromites from within the vein (Fig. 5). Since the vein is so young, there has been no time for in-growth of radiogenic Os. The elevated $^{187}\text{Os}/^{188}\text{Os}$ of the abraded chromite separate (0.1183), (which was a mixture of chromite from both the vein and host) and the abraded powder (0.1296), when compared to the whole rock (0.1120) can only be explained by introduction of radiogenic Os at the time of vein formation, most likely associated with the sulfides.

An estimate of how much Os was added in this fashion can be made if we assume that, before metasomatism, LB-17 had the same $^{187}\text{Os}/^{188}\text{Os}$ as other refractory harzburgites in the suite (i.e., 0.107–0.108), and that the metasomatic magma had $^{187}\text{Os}/^{188}\text{Os}$ of 0.13 to 0.14, the value inferred for rift-related magmas. This suggests that between 12 and 18% of the Os presently in the whole rock was added during metasomatism, corresponding to 0.01 to 0.02 wt.% sulfide addition, assuming 1–2 ppm Os in the sulfide (based on laser ablation ICP-MS data for sulfides in LB-12, Lee et al., unpublished data).

Sample KAT-1 also shows evidence for addition of radio-

genic Os, but has not experienced significant Fe or Re addition; it has the lowest Re/Os of the suite and has low Fe content (7 wt.%). It contains metasomatic glass patches containing clinopyroxene, euhedral olivines (Fo_{92}), skeletal chromites, apatite, phlogopite, harmotome (a Ba zeolite) and sulfides (Fig. 6). Unlike, LB-17, there is no evidence of Fe-enrichment associated with the metasomatism, and the groundmass chromites are large (150–500 μm), round and have thin, euhedral overgrowths with trapped silicate (glass?) inclusions (Fig. 5). The chromite separate has a markedly less radiogenic Os isotopic composition than the whole rock (0.1093 vs. 0.1140), suggesting that the Os composition of the rock has been elevated through addition of radiogenic Os, probably hosted in sulfides found in the glass patches.

In summary, we find evidence for (recent) metasomatic introduction of both Re and radiogenic Os to some of the peridotites from Labait. The Re and Os additions are not coupled, implying that Re is controlled by the silicate fraction whereas Os is brought in with metasomatic sulfides. This observation is in good agreement with empirically derived partition coefficients for Re and Os between sulfide and liquid (Roy-Barman et al., 1998). In samples lacking clear petrographic or chemical evidence for metasomatism it is not clear whether, or to what degree, these processes have occurred.

7. AGE OF THE LITHOSPHERE

The timing of melt depletion in peridotites may be determined from Re-Os systematics in several ways: (1) the rocks may plot on an isochron (e.g. Shirey, 1997), (2) correlations between major elements that are depleted during melting (e.g., Al_2O_3 and CaO) and $^{187}\text{Os}/^{188}\text{Os}$ can be used to infer the age of the melting event from the model age of the intercept on a Al_2O_3 (or CaO) vs. $^{187}\text{Os}/^{188}\text{Os}$ diagram (Reisberg and Lorand, 1995), or (3) model ages may be calculated directly from each peridotite by assuming either all Re measured is secondary (thus the measured $^{187}\text{Os}/^{188}\text{Os}$ represents a minimum age of melt depletion) (T_{RD} ages) or using the measured Re/Os ratio to calculate the time at which the sample had Os isotopic composition equal to a model primitive mantle composition (T_{MA} ages).

For the refractory Labait xenoliths, methods one and two above do not produce reliable results. The lack of correlation of the Labait data on the Re-Os isochron diagram (Fig. 2) is not surprising in light of the evidence for Re-enrichment, Os isotopic overprinting and possible Os depletion described above. This is consistent with previous studies that have shown evidence for recent Re addition in mantle-derived xenoliths (e.g., Meisel et al., 1996; Walker et al., 1989) and disturbed Re/Os in massif peridotites (Reisberg and Lorand, 1995; Reisberg et al., 1991). Moreover, it is not clear that all of the peridotites necessarily formed during one partial melting event (i.e., there is no a priori reason to suppose they should lie on an isochron). Most of the data lie to the right of a 2.8 Ga reference isochron, which corresponds to the oldest T_{RD} ages observed in the suite.

Correlations between indicators of fertility (e.g., Al_2O_3 , CaO, Mg#) and $^{187}\text{Os}/^{188}\text{Os}$ have been observed in massif peridotites and attributed to either mixing between different components (i.e., basalt and harzburgite) (Reisberg et al., 1991) or melt depletion (Reisberg and Lorand, 1995; Reisberg et al.,

1991). If the latter is true, then the y-intercept can be used to determine the initial Os isotopic composition of the peridotites and from this, the timing of melt extraction, hence lithosphere formation. An underlying premise in this approach is that the peridotites in question were originally derived from primitive upper mantle, which has a relatively narrowly defined composition for both major elements and Os isotopes (McDonough and Sun, 1995; Shirey and Walker, 1998).

The good correlation between Al, Ca, and forsterite content with $^{187}\text{Os}/^{188}\text{Os}$ seen in the Labait xenoliths (Fig. 4) cannot be attributed simply to melt extraction, since the trend does not pass through the primitive mantle composition. This leaves two mechanisms which are not mutually exclusive: (1) the trend reflects mixing between ancient, unradiogenic lithosphere and modern, radiogenic asthenospheric mantle, similar to that sampled by the host melilitite and the metasomatic xenoliths (i.e., $^{187}\text{Os}/^{188}\text{Os} = 0.132$ to 0.139), or (2) the range in Os isotopic compositions seen in the xenoliths reflects lithosphere formation during two or more melting events and the trend reflects a secular change in the degree of melt depletion with time. The trend thus cannot be used to determine the age of the lithosphere as has been done for massif peridotites; we return to question of the origin of this trend in the next section.

Given the difficulties cited above with various isochron schemes, we turn to model ages to define the timing of melt extraction beneath Labait. T_{MA} ages (Table 1) generally give unreasonably old ages, due to the high Re/Os ratios (which are a product of recent Re introduction and/or Os loss). T_{RD} ages provide the best estimate of original lithosphere formation, and indicate that the shallowest lithosphere formed at ~ 2.8 Ga. But the highest temperature peridotites, which have Os isotopic compositions (hence T_{RD} ages) intermediate between Archean and modern mantle compositions, are more difficult to interpret.

8. STRUCTURE OF THE LITHOSPHERE

Samples of the shallowest lithospheric mantle beneath Labait are derived from between 80 and 140 km, based on the presence of spinel facies peridotites and equilibration temperatures of the garnet-free, chromite harzburgites (Lee and Rudnick, 1999). In addition to Fe-rich dunites, this mantle section consists of highly refractory spinel, chromite and garnet harzburgites, having very low Al_2O_3 (≤ 0.6 wt.%) and CaO (≤ 0.5 wt.%) and high MgO (> 44 wt.%). The T_{RD} ages of these samples span a relatively narrow range from 2.4 to 2.8 Ga for whole rocks (excluding LB-17 and KAT-1—samples that show evidence for Os isotopic overprinting), with chromite separates for some of these falling mainly in the 2.7 to 2.9 Ga range (Table 2). We include in this group the two garnet-bearing peridotites that have the lowest equilibration temperatures (LB-24 and LB-34) and have bulk compositions more closely resembling the shallower harzburgites than the deep-seated garnet peridotites (Lee and Rudnick, 1999). These samples also have old T_{RD} ages (2.2 to 2.5 Ga). Given the evidence for Os isotopic overprinting cited above, we take the chromite ages of 2.7 to 2.9 Ga as the best estimate of when this portion of the lithosphere formed. It thus appears that a significant thickness of shallow lithosphere (above 140 km) formed at or before ~ 2.8 Ga.

The deepest samples of lithosphere are distinct from the shallower, refractory harzburgites. These deep samples contain garnet, equilibrated over a narrow pressure interval between 4.4 to 4.9 GPa (~ 140 and 160 km), and have deformed textures. They are generally more fertile than the shallower samples, although they are still dominated by harzburgitic (sensu stricto) assemblages (Lee and Rudnick, 1999). Collectively, the deep samples have more radiogenic Os isotopic compositions, corresponding to T_{RD} ages that range from 1 Ga to the future. [Note that the sample yielding the highest pressure (GL4206 at 4.9 GPa or 160 km) is from Dawson et al., 1997, and has not been measured. The next deepest samples come from 4.7 GPa or 150 km depth.] Although the $^{187}\text{Os}/^{188}\text{Os}$ of several of the highest temperature samples overlap those of abyssal peridotites (Fig. 4), our observations from the metasomatic xenoliths and host melilitite suggest the mantle beneath the Tanzanian lithosphere is significantly enriched in $^{187}\text{Os}/^{188}\text{Os}$ compared to a MORB-like mantle source. As discussed above, there are two possible interpretations of these samples: (1) they represent mixtures between the base of the ancient lithosphere and upwelling mantle or melts associated with the rift, and (2) they represent peridotites that experienced melt removal at several different time periods. We discuss each of these hypotheses in turn.

8.1. Mixing at the Base of the Lithosphere

In this scenario, the $^{187}\text{Os}/^{188}\text{Os}$ of the high temperature, deformed garnet peridotites are produced by mixing between unradiogenic Os from the ancient, refractory lithosphere and radiogenic Os from sublithospheric mantle, which has $^{187}\text{Os}/^{188}\text{Os}$ equal to that of the metasomatic xenoliths and host melilitite (0.132 to 0.139). Sample LB-45 may actually be a sample of this sublithospheric mantle. The Os isotopic composition of this mantle is more radiogenic than inferred for MORB source mantle, and is probably derived from a plume-like mantle source.

There are two ways in which such mixing of Os might occur: (1) mixing between a plume-derived silicate melt in the thermal boundary layer at the base of the lithosphere, and (2) mixing and homogenization of sulfide melts at the base of the lithosphere (note that the high temperatures prevalent at these depths are above the sulfide liquidus).

If the high temperature, deformed, garnet peridotites are the product of silicate melt mixing, their higher concentrations of CaO and Al_2O_3 and lower MgO relative to the overlying, refractory peridotites, may also be a product of this mixing (i.e., melt addition). A rough correlation of $^{187}\text{Os}/^{188}\text{Os}$ and $1/\text{Os}$ is observed for some of the garnet peridotites (excluding the two lower temperature samples LB-24 and LB-34 and the low Os concentration sample LB-53). However, the small sample population and the possibility of Os loss, as discussed above, make interpretation of the trend tenuous.

Alternatively, if mixing and homogenization of sulfide melts explains the Os data, then the higher concentrations of CaO and Al_2O_3 , and lower MgO of the high temperature peridotites relative to the overlying, refractory peridotites reflects a lithosphere that was originally stratified with respect to major element composition. Furthermore, for this hypothesis to be viable, the wetting angle (dihedral angle) of sulfide melts must be

sufficiently low to allow their migration along grain boundaries. Recent experimental studies show that the dihedral angle of sulfide melts varies as a function of fO_2 , and that under oxidizing conditions sulfide melts will be mobile (Gaetani and Grove, 1999). Oxidizing conditions under the Tanzanian lithosphere have been suggested by Canil et al. (1994) and can be inferred from the presence of inclusions of Fe-oxides exsolved within sulfide inclusions. The evidence described earlier for Os metasomatism in some of the shallower peridotites is consistent with this inference. However, the fact that the isotopic composition of the single sulfide separate measured from a garnet peridotite is the same as that of the whole rock requires that any sulfide melt percolated into the base of the lithosphere was effectively homogenized with pre-existing Os in these samples. Several of the high temperature garnet peridotites have relatively abundant sulfides (e.g., LB-12, LB-4), which tend to be concentrated within the kelyphitic rims on garnets (Fig. 6), implying sulfide mobility in these samples.

8.2. Multi-stage Growth of the Lithosphere

An alternative hypothesis is that the deepest samples formed through one or more melting events after the ~ 2.8 Ga shallower lithosphere formed. The radiogenic Os isotopic composition for LB-45 suggests it is recently derived from sublithospheric mantle. Its bulk composition is close to that of primitive mantle, with only its higher Mg# reflecting possible melt extraction. If it is indeed lithospheric it must represent a recent addition. The Os isotope compositions of the other deep-seated samples fall between 0.120 and 0.125, corresponding to T_{RD} ages from 1.0 to 0.3 Ga, respectively. This may reflect growth of the lower ~ 20 km of lithosphere at ~ 1 Ga, with the younger T_{RD} ages (0.7 to 0.33 Ga) reflecting variable, time-integrated Re/Os (which is now completely obscured by secondary processes), overprinting at a later time by radiogenic Os and/or discrete melt depletion events in the Proterozoic and Permian, with or without radiogenic Os addition.

In summary, if the high temperature deformed peridotites are not the products of mixing at the base of the lithosphere, then their Os isotopic compositions suggest they are ≤ 1 Ga additions to the lithosphere. Sample LB-45 must be a very recent addition (if it is lithospheric at all). The age of emplacement of the remaining high temperature peridotites is impossible to define precisely, and may range from 1 Ga to present day. No matter when the melting occurred, it must have involved overall lower degrees of melt extraction compared to the 2.8 Ga event, since these high temperature samples are not as refractory as the former.

9. GEODYNAMIC IMPLICATIONS

The data presented here can be used to infer the history of the Tanzanian lithosphere through its 2.8 Ga existence and the possible effects that collisional and rift tectonics may have had on its stability. Archean model ages for lithosphere down to ~ 140 km depth demonstrate that complete delamination of the lithospheric mantle beneath the Tanzanian craton has not occurred. However, 140 km is relatively thin when compared to Archean cratons elsewhere. For example, peridotite xenoliths from the Kaapvaal, Slave, Siberian and Superior cratons derive

from depths of up to ~ 200 km (Boyd and Gurney, 1986; Boyd et al., 1997; Kopylova et al., 1998; Meyer et al., 1994), including xenoliths from the margins of cratons, such as northern Lesotho (e.g., Nixon, 1973). Moreover, even the center of the Tanzanian craton, where diamonds are brought up in Cenozoic kimberlites (Edwards and Howkins, 1966; Nixon, 1987) appears to be at least 200 km thick, on the basis of recent tomographic results (Ritsema et al., 1998). Thus, it is possible that the Archean lithosphere was thicker than at present beneath Labait and that the lowermost lithosphere (≥ 40 km?) was lost by delamination or thermal erosion along the craton margin.

Unfortunately, due to the ambiguities involved in interpreting the ages of the deepest xenoliths (~ 140 to 160 km), it is not possible to determine when this thinning occurred. If these xenoliths are mixtures between a plume and ancient lithosphere, then the thinning is likely to be associated with present-day thermal erosion and rifting. If instead these deep xenoliths represent Proterozoic lithospheric additions, then the thinning must have occurred prior to their formation, and it is possible that delamination (associated with collisional tectonics?) was the cause of the thinning. Finally our data demonstrate that lithospheric mantle thinning beneath the Tanzanian rift has not reached the advanced stages that have been seismically imaged under the Kenyan rift (Prodehl et al., 1994).

10. CONCLUSIONS

The Re-Os data presented here establish that ancient, refractory lithosphere extends to at least ~ 140 km depth beneath the East African Rift in northern Tanzania. This conclusion is in good agreement with recent tomographic images (Ritsema et al., 1998; Nyblade et al., 1999) that show that the Tanzanian lithosphere did not undergo craton-wide delamination or thermal erosion during either the Pan-African collision or Cenozoic rifting. The shallowest portion of the lithosphere beneath Labait (to ~ 140 km depth) is highly refractory with relatively constant Re-depletion ages from chromite separates of 2.5 to 2.9 Ga. Various harzburgites show evidence for recent addition of Re, radiogenic Os, or both. The low sulfur content of all xenoliths suggest the decomposition of sulfides during decompression in the pipe, and may have given rise to some amount of Os depletion in some or all of the xenoliths. The deepest portion of the lithosphere beneath Labait consists of a thin zone (~ 10 – 20 km) of garnet-bearing peridotites that are more fertile, are deformed and have more radiogenic Os compared to the shallower lithosphere. These deep peridotites may be mixtures of ancient lithosphere and underlying plume or may represent younger (1 to 0 Ga) additions to the base of the lithosphere. One sample has major element composition similar to estimates of the primitive mantle. Its $^{187}\text{Os}/^{188}\text{Os}$ (0.133) is radiogenic and overlaps with the range seen for metasomatic xenoliths and the host melilitite. These observations suggest that the asthenospheric mantle beneath the rift has isotopic characteristics of a plume and is distinct from MORB-source mantle.

Complete delamination of the lithospheric mantle has not occurred beneath the Tanzanian craton, but it is possible that thinning occurred on the margin either in the Proterozoic, associated with delamination at a convergent plate boundary or in the Cenozoic, associated with impingement of a plume at the initiation of the East African Rift. Extensive, rift-related thin-

ning, as documented in Kenya, has not yet occurred beneath Tanzania.

Acknowledgments—This work was supported by NSF grant EAR9506510 to Chesley and Rudnick and an N.S.F. graduate fellowship to C.-T. Lee. We are grateful to J. Ruiz, University of Arizona, for support and access to the W. M. Keck foundation NTIMS facility. Kate Tomford and Chris Eckhart are thanked for assistance with sample preparation. Kevin Sharkey and Andy Saunders are thanked for S analyses. David Lange's attention to detail was responsible for the discovery of the Pt alloys. Aloyce Tesha, Andy Nyblade and Dorobo Safari provided invaluable assistance during sample collection. Discussions with W. F. McDonough and K. Righter helped to hone our swords. We appreciate the comments of H.-G. Stosch and two anonymous reviewers, which improved this manuscript. Finally, we thank the Tanzanian government for permission to collect and export samples.

REFERENCES

- Andersen T., Griffin W. L. and O'Reilly S. Y. (1987) Primary sulfide melt inclusions in mantle-derived megacrysts and pyroxenites. *Lithos* **20**, 279–294.
- Bell K. and Dodson M. H. (1980) The geochronology of the Tanzanian shield. *J. Geol.* **89**, 109–128.
- Boyd F. R. and Gurney J. J. (1986) Diamonds and the African lithosphere. *Science* **232**, 472–477.
- Boyd F. R., Pokhilenko N. P., Pearson D. G., Mertzman S. A., Sobolev N. V., and Finger L. W. (1997) Composition of the Siberian cratonic mantle: Evidence from Udachnaya peridotite xenoliths. *Contrib. Mineral. Petrol.* **128**, 228–246.
- Brandon A. D., Creaser R. A., Shirey S. B., and Carlson R. W. (1996) Osmium recycling in subduction zones. *Science* **272**, 861–864.
- Burnham O. M., Rogers N. W., Pearson D. G., van Calsteren P. W., and Hawkesworth C. J. (1998) The petrogenesis of the eastern Pyrenean peridotites: An integrated study of their whole-rock geochemistry and Re-Os isotope composition. *GCA* **62**: 2293–2310.
- Burton K. W., Schiano P., Birck J.-L., and Allègre C. J. (1998) The behaviour of Re and Os in mantle minerals with implications for mantle melting. *Eos*, S373.
- Canil D., O'Neill H. St. C., Pearson D. G., Rudnick R. L., McDonough W. F., Carswell D. A. (1994) Ferric iron in peridotites and mantle oxidation states. *Earth Planet. Sci. Lett.* **123**, 205–220.
- Carlson R. W. and Irving A. J. (1994) Depletion and enrichment history of subcontinental lithospheric mantle: An Os, Sr, Nd and Pb isotopic study of ultramafic xenoliths from the northwestern Wyoming Craton. *Earth and Planetary Science Letters* **126**, 457–472.
- Carlson R. W., Pearson D. G., Boyd F. R., Shirey S. B., Irvine G., Menzies A. H. and Gurney J. J. (1999a) Re-Os systematics of lithospheric peridotites: Implications for lithosphere formation and preservation. In *Proc. 7th Internat. Kimberlite Conf.*, (ed. J. J. Gurney and S. R. Richardson), (in press).
- Carlson R. W., Irving A. J. and Hearn B. C. (1999b) Chemical and isotopic systematics of peridotite xenoliths from the Williams Kimberlite, Montana: Processes of lithosphere formation, modification and destruction. In *Proc. 7th Internat. Kimberlite Conf.*, (ed. J. J. Gurney and S. R. Richardson), (in press).
- Chesley J. T. and Ruiz J. (1998) Crust-mantle interaction in large igneous provinces: Implications from the Re-Os isotope systematics of the Columbia River flood basalts. *Earth Planet. Sci. Lett.* **154**, 1–11.
- Cohen A. S. and Waters F. G. (1996) Separation of osmium from geologic materials by solvent extraction for analysis by TIMS. *Anal. Chim. Acta* **332**, 269–275.
- Creaser R., Papanastassiou D., and Wasserburg G. (1991) Negative thermal ion mass spectrometry of osmium, rhenium and iridium. *Geochim. Cosmochim. Acta* **55**, 397–401.
- Dawson J. B. (1992) Neogene tectonics and volcanicity in the North Tanzania sector of the Gregory Rift Valley: Contrasts with the Kenya sector. *Tectonophysics* **204**, 81–92.
- Dawson J. B., James D., Paslick C., and Halliday A. M. (1997) Ultrabasic potassic low-volume magmatism and continental rifting in north-central Tanzania: Association with enhanced heat flow. *Proc. Sixth Int. Kimberlite Conf., Russian Geology and Geophysics* **38**, 69–81.
- Ebinger C., Poudjom Djomani Y., Mbede E., Foster A., and Dawson J. B. (1997) Rifting Archaean lithosphere: The Eyasi-Manyara-Natron rifts, East Africa. *J. Geol. Soc.* **154**, 947–960.
- Edwards C. B. and Howkins J. B. (1966) Kimberlites in Tanganyika with special reference to the Mwadui occurrence. *Econ. Geol.* **61**, 537–554.
- Gaetani G. A. and Grove T. L. (1999) Wetting of mantle olivine by sulfide melt: Implications for Re/Os ratios in mantle peridotite and late-stage core formation. *Earth Planet. Sci. Lett.* (in press).
- Handler M. R., Bennett V. C., and Esat T. M. (1997) The persistence of off-cratonic lithospheric mantle: Os isotopic systematics of variably metasomatised southeast Australian xenoliths. *Earth Planet. Sci. Lett.* **151**, 61–75.
- Hart S. R. and Ravizza G. E. (1996) Os partitioning between phases in lherzolite and basalt. In *Earth Processes. Reading the Isotopic Code* (ed. A. Basu and S. R. Hart) Geophys. Monograph **95**, Am. Geophys. Union, 123–134.
- Houseman G. A., McKenzie D. P., and Molnar P. (1981) Convective instability of a thickened boundary layer and its relevance for the thermal evolution of continental convergent belts. *J. Geophys. Res.* **86**, 6115–6132.
- Keays R. R., Sewell D. K. B., Mitchell R. H. (1981) Platinum and palladium minerals in upper mantle-derived lherzolites. *Nature* **294**, 646–648.
- Kopylova M. G., Russell J. K., and Cookenboo H. (1998) Upper-mantle stratigraphy of the Slave craton, Canada: Insights into a new kimberlite province. *Geology* **26**, 315–319.
- Lee C.-T. and Rudnick R. L. (1999) The significance of carbonate inclusions in mantle rocks: Petrochemical investigation of calcites in peridotite xenoliths from northeastern Tanzania, Contrib. Mineral. Petrol. (submitted).
- Lee C.-T. and Rudnick R. L. (1999) Compositionally stratified cratonic lithosphere: Petrology and geochemistry of peridotite xenoliths from the Labait tuff cone, Tanzania. In *Proc. 7th Internat. Kimberlite Conf.*, (ed. J. J. Gurney and S. R. Richardson), (in press).
- Lorand J. P. (1989) Abundance and distribution of Cu-Fe-Ni sulfides, sulfur, copper and platinum-group elements in orogenic-type spinel lherzolite massifs of Ariège (northeastern Pyrenees, France). *Earth Planet. Sci. Lett.* **93**, 50–64.
- Lorand J. P. (1990) Are spinel lherzolite xenoliths representative of the abundance of sulfur in the upper mantle? *Geochim. Cosmochim. Acta* **54**, 1487–1492.
- Marcantonio F., Zindler A., Reisberg L., and Mathez E. A. (1993) Re-Os isotopic systematics in chromites from the Stillwater Complex, Montana, USA. *Geochim. Cosmochim. Acta* **57**, 4029–4037.
- McCandless T. E. and Ruiz J. (1991) Osmium isotopes and crustal sources for platinum group mineralization in the Bushveld complex, South Africa. *Geology* **19**, 12225–12228.
- McDonough W. F. and Frey F. A. (1989) Rare earth elements in upper mantle rocks. In *Geochemistry and Mineralogy of Rare Earth Elements* (ed. B. R. Lipin and G. A. McKay), Vol. 21, pp. 99–145. Mineralogical Society of America.
- McDonough W. F. and Sun S.-s. (1995) Composition of the earth. *Chem. Geol.* **120**, 223–253.
- Meisel T., Walker R. J., and Morgan J. W. (1996) The osmium isotopic composition of the Earth's primitive upper mantle. *Nature* **383**, 517–520.
- Meyer H. O. A., Waldman M. A., and Garwood B. L. (1994) Mantle xenoliths from kimberlite near Kirkland Lake, Ontario. *Can. Mineral.* **32**, 295–306.
- Möller A., Appel P., Mezger K., and Schenk V. (1995) Evidence for a 2 Ga subduction zone: Eclogites in the Usagaran belt of Tanzania. *Geology* **23**, 1067–1070.
- Möller A., Mezger K., and Schenk V. (1998) Crustal age domains and the evolution of the continental crust in the Mozambique belt of Tanzania: Combined Sm-Nd, Rb-Sr and Pb-Pb isotopic evidence. *J. Petrol.* **39**, 749–783.
- Nixon P. H. (1973) *Lesotho Kimberlites*. Lesotho National Development Corporation.
- Nixon P. H. (1987) *Mantle Xenoliths*. John Wiley & Sons.

- Nyblade A. A., Birt C., Langston C. A., Owens T. J., and Last R. J. (1996) Seismic experiment reveals rifting of the craton in Tanzania. *Eos* **77**, 517–521.
- Nyblade A. A., Pollack H. N., Jones D. L., Podmore F., and Mushayandebvu M. (1990) Terrestrial heat flow in East and Southern Africa. *Journal of Geophysical Research* **95**, 17371–17384.
- Nyblade A. A., Owens T. J., Langston C. A., Battenhouse T. R., Gurrola H. and Ritsema J. (1999) Upper mantle structure beneath east Africa and the origin of Cenozoic extensional tectonism, EOS 1999 Spring Meeting, S215.
- Olive V., Ellam R. M., and Harte B. (1997) A Re-Os isotope study of ultramafic xenoliths from the Matsoku kimberlite. *Earth Planet. Sci. Lett.* **150**, 129–140.
- Pearson D. G., Carlson R. W., Shirey S. B., Boyd F. R., and Nixon P. H. (1995a) The stabilisation of Archaean lithospheric mantle: A Re-Os isotope study of peridotite xenoliths from the Kaapvaal craton. *Earth Planet. Sci. Lett.* **134**, 341–357.
- Pearson D. G., Shirey S. B., Carlson R. W., Boyd F. R., Pokhilenko N. P., and Shimizu N. (1995b) Re-Os, Sm-Nd, and Rb-Sr isotope evidence for thick Archaean lithospheric mantle beneath the Siberian craton modified by multi-stage metasomatism. *Geochim. Cosmochim. Acta* **59**, 959–977.
- Prodehl C., Keller G. R., and Khan M. A. (1994) Crustal and upper mantle structure of the Kenya rift. *Tectonophysics (spec. issue)* **2366**, 1–483.
- Reisberg L. and Lorand J.-P. (1995) Longevity of sub-continental mantle lithosphere from osmium isotope systematics in orogenic peridotite massifs. *Nature* **376**, 159–162.
- Reisberg L. C., Allègre C. J., and Luck J. M. (1991) The Re-Os systematics of the Ronda Ultramafic Complex of southern Spain. *Earth Planet. Sci. Lett.* **105**, 196–213.
- Ritsema J., Nyblade A. A., Owens T. J., Langston C. A., and VanDecar J. C. (1998) Upper mantle seismic velocity structure beneath Tanzania, East Africa: Implications for the stability of cratonic lithosphere. *J. Geophys. Res.* **103**, 21201–21213.
- Roy-Barman M. and Allègre C. J. (1995) $^{187}\text{Os}/^{186}\text{Os}$ ratios of mid-ocean ridge basalts and abyssal peridotites. *Geochim. Cosmochim. Acta* **58**, 5043–5054.
- Roy-Barman M., Wasserburg G. J., Papanastassiou D. A. and Chaussidon M. (1998) Osmium isotopic compositions and Re-Os concentration in sulfide globules from basaltic glasses. *Earth Planet. Sci. Lett.* **154**, 331–347.
- Rudnick R. L., Ireland T. R., Gehrels G., Irving A. J., Chesley J. T., and Hancher J. M. (1999) Dating mantle metasomatism: U-Pb geochronology of zircons in cratonic mantle xenoliths from Montana and Tanzania. In *Proceedings Seventh International Kimberlite Conference*, (ed. J. J. Gurney and S. R. Richardson), (in press).
- Shirey S. B. (1997) Initial osmium isotopic composition of Munro Township, Ontario, komatiites revisited: Additional evidence for near-chondritic late-Archaean convecting mantle beneath the Superior Province. *7th Ann. V. M. Goldschmidt Conf. LPI Contrib.* **921**, 193.
- Shirey S. B. and Walker R. J. (1995) Carius tube digestions for low blank rhenium-osmium analysis. *Analyt. Chem.* **67**, 2136–2141.
- Shirey S. B. and Walker R. J. (1998) Re-Os isotopes in cosmochimistry and high-temperature geochemistry. *Ann. Rev. Earth Planet. Sci.* **26**, 423–500.
- Spera F. J. (1980) Aspects of magma transport. In *Physics of Magmatic Processes* (ed. R. B. Hargraves), pp. 265–323 Princeton Univ. Press.
- Snow J. E. and Reisberg L. (1995) Os isotopic systematics of the MORB mantle: Results from abyssal peridotites. *Earth Planet. Sci. Lett.* **133**, 411–421.
- Volkening J., Walczyk T., and Heumann K. G. (1991) Osmium isotope ratio determinations by negative thermal ionization mass spectrometry. *Int. J. Mass Spect. Ion Proc.* **105**, 147–159.
- Walker R. J., Carlson R. W., Shirey S. B., and Boyd F. R. (1989) Os, Sr, Nd, and Pb isotope systematics of southern African peridotite xenoliths: Implications for the chemical evolution of the subcontinental mantle. *Geochim. Cosmochim. Acta* **53**, 1583–1595.

APPENDIX

Petrographic Descriptions

Key to mineral abbreviations: Chr = chromite, Cpx = Cr-diopside, Ol = olivine, Opx = orthopyroxene, Phlog = phlogopite, Sp = spinel. Minerals are listed in order of relative abundance. Mg# refers to bulk rock Mg#, Fo refers to forsterite content of olivines.

Garnet-free harzburgites

KAT-1: Ol–Opx–Chr–Cpx

Mg# = 92.1

Fresh, coarse-granular texture; round primary chromites with euhedral overgrowths; glassy patches contain euhedral olivine, skeletal chromites, apatite, phlogopite, harmotome (a Ba zeolite) and sulfides.

LB 1: Ol–Opx–Chr–Phlog

Mg# = 93.0

Fresh; coarse-granular texture; round primary chromites with euhedral overgrowths; Opx–Sp patches contain glass and wormy spinels; sulfides occur as inclusions in Ol and as elongate blebs and small irregular grains associated with Phlog.

LB 9: Ol + Opx + Chr

Mg# = 92.9

Moderately fresh; coarse granular; bright, rusty orange material in secondary veins (devitrified glass); isotropic, green glass present also; large Ol grains with feathery grain boundaries (alteration); Opx is small; fresh, round chromites included in Ol; tiny sulfides in glass and veins; trace amounts of Fe-oxides; melt patches contain euhedral Ol, Sp, rare Cpx, and possible apatite; perovskite on grain boundaries; Similar to KAT-1 except chromites have smooth surfaces—no evidence of overgrowth.

LB 14: Ol–Opx–Chr–Cpx–Phlog

Mg# = 92.4

Fresh; fine-grained; Cpx is secondary; Cpx–Phlog intergrowths common; Opx occurs as small grains; chromites are skeletal and surrounded by Phlog, Cpx, euhedral Ol and glass; no sulfide observed.

LB 16: Ol–Opx–Cpx–Chr

Mg# = 92.0

Fresh; fine-grained recrystallized texture; Chromites rimmed by patches of Opx, Ol, Cpx, Phlog, euhedral Sp, glass; exsolution in Opx; some Cpx appears primary; sulfides rare; Harmotome in glass patches.

LB 17: Ol–Opx–Chr–Phlog–Rut–Zircon–Sulfide

Mg# = 91.5

Moderate alteration on grain boundaries; medium-grained; rock consists of a cross-cutting planar Opx-rich vein (Opx + Chr + Phlog + Rut + Zircon + Sulfide + CO₂); host rock contains Ol + Opx + Chr; fluid inclusions abundant in vein; chromites outside of vein are skeletal and surrounded by glass patches. Chromites in vein contain CO₂ and sulfide inclusions.

Garnet-bearing peridotites

LB 4: Ol–Opx–former Gt–Cpx

Mg# = 91.1

Moderately fresh; porphyroclastic texture; Ol fine-grained; rims of Cpx are cloudy; former Gt patches consist of coarse outer corona (Opx + cpx + sp intergrowths) and fine interior kelyphite; sulfides abundant in Gt coronas and disseminated throughout sample—mainly on Ol subgrain boundaries; irregular, interstitial Fe-oxides; Ol inclusions in former Gt.

LB 24: Ol–Opx–former Gt–Cpx

Mg# = 92.2

Altered; medium to coarse-grained; Cpx primary, but with altered rims; former Gt patches consist of Sp + Opx coronas and fine-grained kelyphitic core; rare sulfides in Gt coronas; small perovskites in veins.

LB 12: Ol–Opx–Gt–Cpx

Mg# = 90.0

Mostly fresh; slight grain boundary alteration; fine-grained texture; awesome!; most garnet has decomposed to coarse-grained corona (Opx + Cpx + Sp symplectite) and fine-grained kelyphitic core, but a few are preserved beautifully; Cpx is primary (large round grains); abundant sulfides occur as small round inclusions in Ol and as large round

sulfides in Gt coronas; platinum alloy was observed in oxide breakdown patches within a sulfide inside a Gt corona.

LB 34: Ol–Opx–former Gt–Cpx–Phlog–Mg–Ilmenite

Mg# = 89.8

Fresh; coarse-grained porphyroclastic texture; recrystallized grain boundaries; decomposed garnet patches with coronas of Sp + Opx + Cpx, fine-grained kelyphitic cores, and Ol inclusions; matrix is Ol + Opx + Cpx; most cpx occurs in patches, veins, or on grain boundaries; Cpx rims are cloudy due to alteration and fluid inclusions; some Opx rimmed entirely by Cpx; fine-grained Phlog common; veins of orange material (former glass?); some Opx recrystallized into patches with Cpx.

LB-45 Ol–former Gt–Cpx–Opx

Mg# = 89.2

Fresh; medium-grained Ol forms foliated groundmass with tabular to mosaic texture; rare, Opx porphyroclasts; Cpx is abundant and has thin decompression rims; Gt replaced by coarse-grained spinel and pyroxene intergrowths, occasionally with finer-grained, kelyphitic interiors; tabular Ol included in Gt; sulfides very rare; occasional Fe-oxides mark former sulfides?

LB 50: Ol–Opx–former Gt–Cpx

Mg# = 91.0

Moderate alteration; fine-grained, porphyroclastic texture; Gt has decomposed into symplectic intergrowth of Sp + Opx from rim to core; most Cpx is large; tiny sulfides in former Gt.

LB 53: Ol–Opx–Gt–Cpx

Mg# = 90.8

Alteration on grain boundaries; fine-grained mosaic-porphyroclastic texture; Ol and pyroxenes in groundmass appear recrystallized; matrix grains granular (triple junctions); some Gt is fresh, but all have reaction rim of Sp + Opx; tiny sulfide in Gt-breakdown patches.

KAT 17: Ol–Opx–Cpx–Gt

Mg# = 88.0

Foliated texture defined by aligned Cpx and recrystallized Ol; some large, deformed Ol porphyroclasts remain; Gt has reaction corona of Sp + pyroxene and fine-grained kelyphite inner rim around pristine core; Cpx characterized by alteration/decompression rims; tiny sulfides in recrystallized Ol and in Gt corona.

Spinel Peridotites

LB 11: Ol–Opx–Sp–Cpx

Mg# = 92.0

Slight alteration; fine-grained; Opx and Cpx are all small; Cpx

mostly secondary; primary Cpx show some alteration; Opx has exsolution lamellae of opx(?). Chr/Sp rimmed by Cpx + glass; euhedral rim overgrowths on chromite; rare sulfides in Ol and occasionally in alteration patches.

Pyroxenite

LB 15: Ol + Cpx

Mg# = 87.0

Fresh; medium-grained; large, primary Cpx; all Cpx have spongy rims due to pervasive fluid inclusions; some have exsolution lamellae; Fe-oxides rare (ilmenite on Cpx rims).

Glimmerite

LB 49: Phlog + Cpx

Mg# = 81.9

Fresh; Medium to fine-grained Phlog with interstitial ilmenite and rare Cpx; ilmenite also occurs as lamellae within Phlog; no sulfides observed.

Fe-rich Dunites

KAT 5: Ol + Chr

Fo = 86.4

Medium- to coarse-grained Ol with decorated grain boundaries (alteration?); pale brown exsolution lamellae in Ol; small ($\leq 50 \mu\text{m}$), rounded Chr in planar arrays within Ol; some Chr have high reflectivity rims (rutile?); rare, tiny ($\leq 6 \mu\text{m}$) sulfides in Ol.

KAT 12: Ol + Cpx

Fo = 85.9

Coarse-grained Ol with small ($\leq 250 \mu\text{m}$), rounded clinopyroxenes that are riddled with inclusion of CO_2 , sulfide and chromite; rare perovskite on grain boundaries; small, euhedral chromites with high reflectivity rims (rutile?) occur in glass patches.

KAT 14: Ol + Cpx + Chr

Fo = 86.7

Medium- to coarse-grained Ol with large, elongated Chr; Cpx rims Chr.

LB 59: Ol + Phlog

Fo = 84.7

Moderately fresh; medium-grained; extensive secondary Phlog forming interconnected networks and veins along grain boundaries; tiny sulfides + Fe-oxides present with Phlog.